

OCTOBER 01 2005

Matched field range and depth resolution in range-dependent waveguides

Brian H. Tracey



ARLO 6, 274–279 (2005)

<https://doi.org/10.1121/1.2006247>



View
Online



Export
Citation

CrossMark

Related Content

Matched field inversion with a moving source in a shallow-water environment

J Acoust Soc Am (November 2000)

Array design and motion effects for matched field processing

J Acoust Soc Am (November 2000)

Statistical description of matched field processing ambiguity surfaces

J. Acoust. Soc. Am. (September 2005)



ASA

Advance your science and career as a member of the
Acoustical Society of America

[LEARN MORE](#)

Matched field range and depth resolution in range-dependent waveguides

Brian H. Tracey

MIT Lincoln Laboratory, 244 Wood St., Lexington, MA 02420
btracey@neurometrix.com

Abstract: Estimates of range and depth resolution are required in order to determine computational grid spacings for matched field processing (MFP). In this paper it is shown how previous results for range-independent waveguides can be extended to account for range dependence by using standard adiabatic formulations. Significant differences in MFP resolution are observed for up-slope versus down-slope propagation due to changes in the path-integrated attenuation loss. MFP resolution is set by multipath interference lengths, so resolution estimates also relate to expected spatial scales for transmission loss fading.

© 2005 Acoustical Society of America

PACS numbers: 43.30.Wi [RR]

Date Received: December 5, 2004 Date Accepted: September 1, 2005

1. Introduction

Methods for estimating the range and depth resolution of conventional matched field processing (MFP) are explored in this paper. MFP uses propagation models to predict the pressure fields that would be caused by sources on a three-dimensional search grid. These predicted fields are correlated against the received data, and peaks in the output are used to identify possible source locations.¹ While exact resolution values are often not needed, “rules of thumb” are very useful in deciding how finely to grid up the environment. The discussion below shows that previously published rules of thumb can be extended to range-dependent waveguides in a fairly straightforward manner.

MFP exploits the structure of the acoustic field caused by interference between multipath components. Thus MFP resolution is determined by the interference length scales for the propagating multipath components. Understanding these length scales is useful for sonar applications other than matched field processing. For example, transmission loss fades also occur on length scales set by multipath interference.

2. Rules of thumb for range-independent waveguides

The acoustic field can often be usefully described as a sum of normal modes.² These modes are standing waves in the depth dimension that propagate in range with horizontal wave numbers k_n . The mode shapes in depth are determined by interference between up-and down-going plane waves, propagating with vertical wave numbers given by

$$k_{zn}(z) = \sqrt{k_0^2(z) - k_n^2}, \quad (1)$$

where $k_0(z)$ is the medium wave number $\omega/c(z)$. Both k_0 and k_n are functions of depth because the sound speed changes with depth. The number of modes supported by the waveguide depends on the ocean depth and frequency.

Several early MFP papers used mode interference lengths to give simple rules of thumb for resolution in range-independent environments. Wilson *et al.*³ argued that an achievable range resolution is set by the smallest mode interference length. The interference in range between two modes is proportional to $e^{i(k_n - k_m)r}$, giving a range interference wavelength of $2\pi/(k_n - k_m)$. Thus, the smallest interference length is

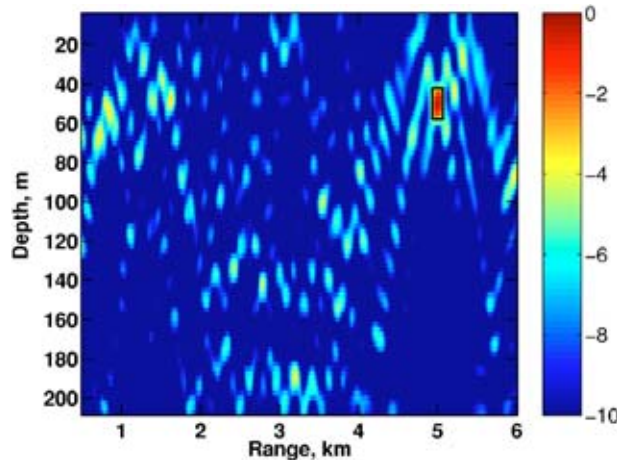


Fig. 1. Example CMFP ambiguity surface with superimposed rule of thumb result. The array, environment, and frequency (112 Hz) are taken from SBCX. Color bar values are power in dB.

$$L_R \approx \frac{2\pi}{\max(k_n - k_m)} \tag{2}$$

Shang⁴ suggested that MFP depth resolution is proportional to the water depth divided by the highest mode number. This distance is proportional to the average distance between zero crossings of the highest mode.

The results above can be restated by noting that since the mode wave numbers generally increase monotonically, the range resolution is given by

$$L_R \approx \frac{2\pi}{k_1 - k_M}, \tag{3}$$

where k_1 is the wave number for mode 1 and k_M is the wave number for mode M , the highest propagating mode with significant energy. Similarly, the depth resolution can be expressed as

$$L_z(z) \approx \frac{2\pi}{2k_{zM}(z)}, \tag{4}$$

where k_{zM} is the vertical wave number for mode M and z is the depth of interest. This expression is equivalent to Shang’s criterion when mode shapes are sinusoidal. Depth resolution is set by interference between up- and down-going waves for the highest mode supported, just as the range resolution is determined by interference mode 1 and the highest mode M .

These rules of thumb require choosing the highest significant mode. This can be done by calculating the modal attenuations at the range of interest. Losses of higher modes are compared to that of the least attenuated mode, which is generally mode 1. The criterion used here is that “significant” modes suffer attenuation losses that are within 10 dB of the least attenuated mode’s loss.

A test of this rule of thumb is shown in Fig. 1. This example is for a vertical array consisting of 30 elements spaced at 5.8 m separation, modeled on those used in the Santa Barbara Channel experiment (SBCX).⁵ Conventional MFP output power is plotted versus range and depth for a source at 5 km range and 50 m depth. The simulation frequency is 112 Hz (a projected tone used in SBCX) with no environmental mismatch present. In this plot (and in following plots) the output is normalized to give 0 dB at the source location. The resolution estimates from the modal rule of thumb are shown as a “box” of size $L_R \times L_z$ overlaid on the

source position. The agreement between simulation and prediction is surprisingly good considering that a half-power criterion is not specifically used in determining the rule of thumb. Simulations for a range of environments show a similar agreement.

3. Extension to adiabatic range-dependence

The references cited above assumed that the ocean is range independent. In reality the ocean is always range dependent, at least to some extent, due to variations in oceanography and water depth. In this section the results above are extended to the case where range dependence can be described by adiabatic normal modes.

The adiabatic normal mode formulation assumes that range variations in the ocean are sufficiently gentle that the coupling of energy between modes can be neglected.² For a sensor at $\mathbf{r}_i=(0, 0, z_i)$, the Green's function is given by

$$G(f, \mathbf{r}_i) = \frac{ie^{-i\pi/4}}{\rho(z_s)\sqrt{8\pi}} \sum_{n=1}^N \psi_n(z_s, r_s) \psi_n(z, 0) \frac{e^{-i\int_0^{r_s} k_n(r') dr'}}{\sqrt{\int_0^{r_s} k_n(r') dr'}} \tag{5}$$

where ψ_n and k_n are, respectively, the mode shapes and mode horizontal wave numbers at the frequency f , z_s is the source depth, and r_s is the source-receiver range. The mode shapes and mode horizontal wave numbers are allowed to vary with range, but coupling between modes is not allowed. If mode n is cut off at some range, for example because it is no longer supported at a new ocean depth, the energy from this mode is assumed to be lost.

Regardless of range dependence, MFP acts to backpropagate the acoustic field to the source location. Thus the range and depth resolution is set by the modal wave numbers at the source location. The effect of the adiabatic propagation is to change the attenuation per mode integrated along the path, thus potentially changing the number of significant modes. For example, high-order modes excited by a source in deep water may be cut off as they propagate up-slope to a receive array. If the array does not receive these modes, it cannot backpropagate them to the source location. The spread in backpropagated wave numbers is therefore reduced (compared to a flat ocean) and resolution is reduced.

The range-averaged attenuation for mode m is calculated as

$$\alpha_m^{av} = \int_0^{r_s} \alpha_m(r') dr' = \sum_{k=1}^P \alpha_m[k] \Delta r_k \tag{6}$$

where r_s is again the source-receiver range. The summation shown assumes that P range-independent segments, each of range extent Δr_k , are used to approximate the continuously varying ocean between source and receiver. If a mode is cut off in some range segment its attenuation α_m is taken to be infinity. As above, the highest mode L is calculated as the highest-order mode whose loss is within 10 dB of the least attenuated mode. The range and depth resolution are then found from

$$L_R \approx \frac{2\pi}{k_1(r_s) - k_L(r_s)}, \tag{7}$$

$$L_Z \approx \frac{\pi}{k_{zL}(r_s, z)}.$$

The changes from Eqs. (3) and (4) are that the wave numbers are range dependent, and that the highest significant mode L is modified due to range-dependent attenuation.

To test this calculation, examples of down-slope and up-slope MFP are shown in Figs. 2 and 3. The SBCX seabed parameters and sound speed profile are again assumed (with the measured sound speed profile extrapolated linearly, as needed). Vertical line arrays spanning

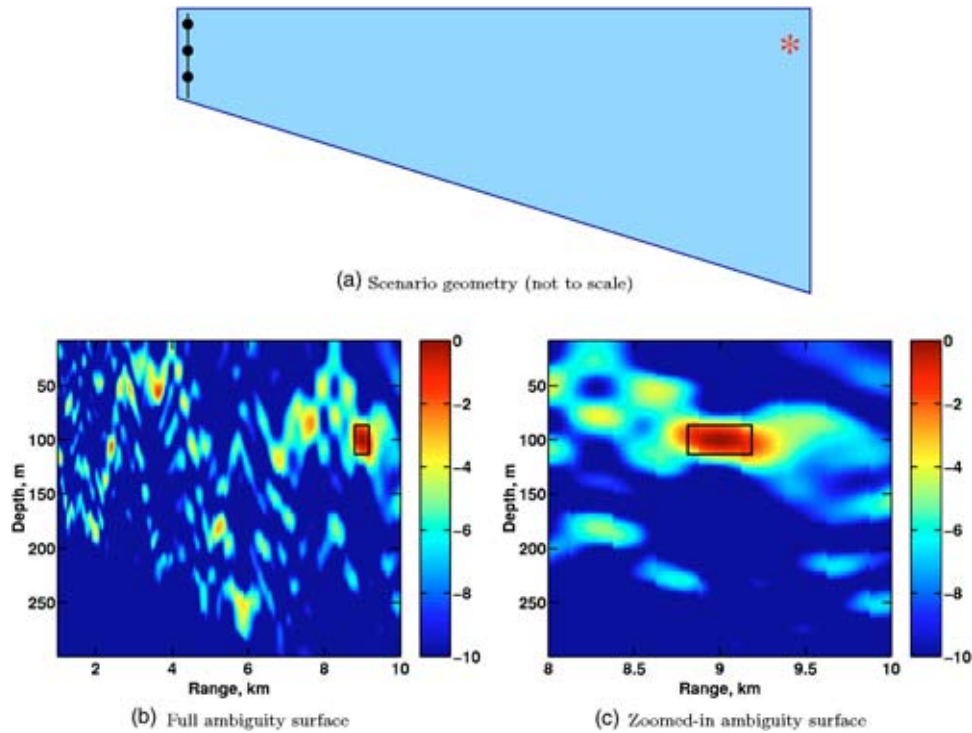


Fig. 2. Adiabatic result for up-slope VLA looking at a down-slope source, 112 Hz. Resolution estimates are overlaid in black. Increased attenuation due to up-slope propagation leads to decreased range and depth resolution and higher sidelobes. Color bar values are power in dB.

nearly the full water column are located at $r=0$ in both plots, and a source is located at 9 km range and 100 m depth. The ocean depth varies between 150 and 350 m over the ranges shown. Main lobe sizes estimated using Eq. 7 are superimposed on the plot.

The plots show several interesting features. In Fig. 2 the array is looking down-slope, meaning the acoustic energy has propagated up-slope to reach the array. Modal cutoff effects due to changing water depth have stripped a number of high-order modes from the field. This results in decreased range and depth resolution. It also results in increased sidelobe levels, as fewer multipaths can be added to resolve ambiguous source locations. Figure 3, in which the array is looking up-slope (so energy is propagating down-slope to the array), shows the opposite trend. Much finer range and depth resolution and lower sidelobe levels are seen.

Figure 4 compares two zoomed-in ambiguity surfaces in the neighborhood of the source location. Figure 4(a) repeats the result from Fig. 3, in which an offshore array is looking up toward a shallow source. Figure 4(b) shows the expected result for an array located at 150 m, looking *across* the slope toward the source (horizontal refraction is ignored). Both resolution and sidelobes are improved for the array that is farther offshore, due to lower attenuation as sound propagates down-slope.

As a practical note, successful MFP requires accurate environmental information. While Fig. 4 suggests that better performance could be obtained when looking up-slope than when looking across-slope, errors in modeling bathymetry could easily counteract this advantage.

4. Summary

Estimates of range and depth resolution are required when setting up the computational search grid for matched field processing (MFP). In this paper, earlier results are extended to give reso-

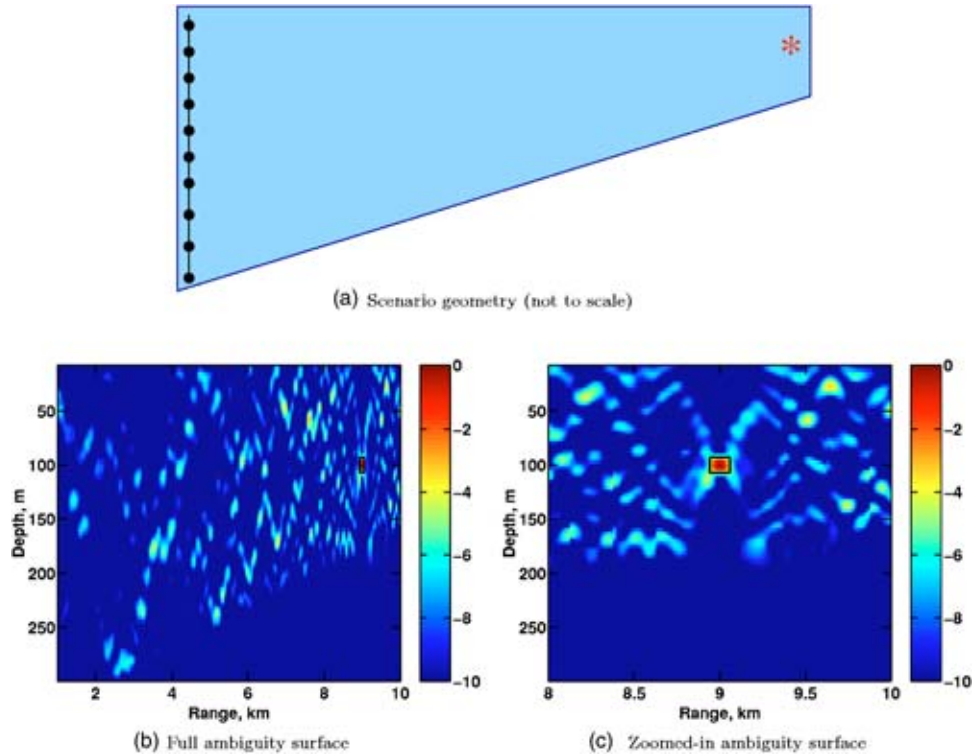


Fig. 3. Adiabatic result for down-slope VLA looking at an up-slope source, 112 Hz. Resolution estimates are overlaid in black. Mode attenuation is less in this geometry, leading to finer-scale range and depth resolution and lower sidelobes. Color bar values are power in dB.

lution estimates in range-varying environments. The simulation examples show that both resolution and sidelobe levels are improved for an offshore array looking up-slope toward a noise source, though achieving this improvement with data would require excellent bathymetric information.

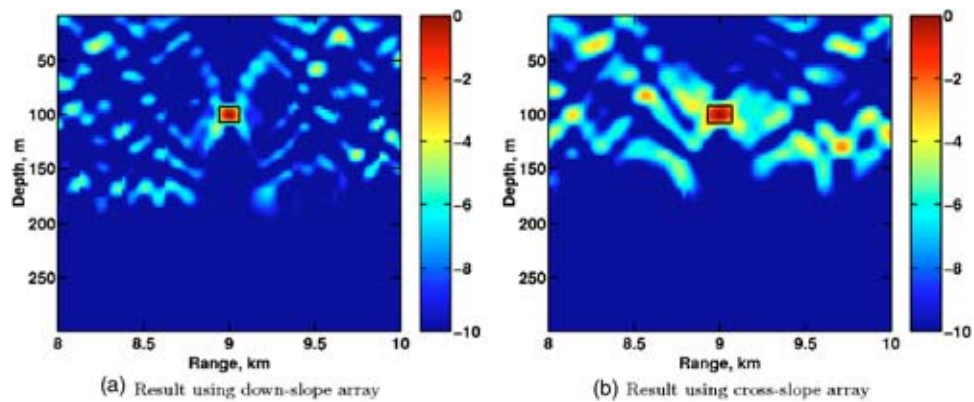


Fig. 4. Zoomed-in results comparing localization of a source at the 150 m depth contour using arrays oriented down-slope and cross-slope from the source. Color bar values are power in dB.

24 September 2023 18:08:20

Acknowledgments

The author would like to thank his co-workers Nigel Lee, Lisa Zurk, and Bill Payne for helpful discussions on this topic. Suggestions made by the reviewers are also gratefully acknowledged. This work was sponsored by DARPA-ATO under Air Force Contract No. F19628-00-C-0002. Opinions, interpretations, conclusions, and recommendations are those of the author and are not necessarily endorsed by the United States Government.

References and links

- ¹A. Baggeroer, W. Kuperman, and P. Mikhalevsky, "An overview of matched field methods of ocean acoustics," *IEEE J. Ocean. Eng.* **18**, 401–424 (1993).
- ²F. Jensen, W. Kuperman, M. Porter, and H. Schmidt, *Computational Ocean Acoustics* (American Institute of Physics, New York, 1993).
- ³G. Wilson, R. Koch, and P. Vidmar, "Matched mode localization," *J. Acoust. Soc. Am.* **84**, 310–320 (1988).
- ⁴E. C. Shang, "Source depth estimation in waveguides," *J. Acoust. Soc. Am.* **77**, 1413–1418 (1985).
- ⁵L. Zurk, N. Lee, and J. Ward, "Source motion mitigation for adaptive matched field processing," *J. Acoust. Soc. Am.* **113**, 2719–2731 (2003).